



Liu, W. and Geroliminis, N. (2017) Doubly dynamics for multi-modal networks with park-and-ride and adaptive pricing. *Transportation Research Part B: Methodological*, 102, pp. 162-179. (doi:[10.1016/j.trb.2017.05.010](https://doi.org/10.1016/j.trb.2017.05.010))

This is the author's final accepted version.

There may be differences between this version and the published version. You are advised to consult the publisher's version if you wish to cite from it.

<http://eprints.gla.ac.uk/141561/>

Deposited on: 24 May 2017

Enlighten – Research publications by members of the University of Glasgow
<http://eprints.gla.ac.uk33640>

Doubly Dynamics for Multi-modal Networks with Park-and-ride and Adaptive Pricing

Wei Liu^{a,b,*}, Nikolas Geroliminis^b

^a *School of Engineering, University of Glasgow, Glasgow G12 8LT, United Kingdom*

^b *Urban Transport Systems Laboratory (LUTS), École Polytechnique Fédérale de Lausanne (EPFL), CH-1015 Lausanne, Switzerland*

Abstract

This paper models and controls a multi-region and multi-modal transportation system, given that the travelers can adjust their mode choices from day to day, and the within-day traffic dynamics in the network also evolve over days. In particular, it considers that the city network can be partitioned into two regions (center and periphery). There are park-and-ride facilities located at the boundary between the city center region and the periphery. Travelers can either drive to the city center, or take public transit, or drive to the park-and-ride facilities and then transfer to the public transit. Travelers can “learn” from their travel experience, as well as real-time information about traffic conditions, thus will adjust their choices accordingly. It follows that the dynamic traffic pattern (within-day) in the city network will evolve over (calendar) time (day-to-day). To improve traffic efficiency in the network, an adaptive mechanism, which does not need detailed travelers’ behavioral characteristics, is developed to update parking pricing (or congestion pricing) from period to period (e.g., one period can be one month). The developed doubly dynamics methodological framework coupled with a feedback pricing mechanism unfolds and influences equilibrium system characteristics that traditional static day-to-day models cannot observe. The proposed adaptive pricing approach is practical for implementation in large-scale networks as the variables involved can be observed in real life with monitoring techniques. Also, it can contribute to reduce total social cost effectively, as shown in the numerical experiments.

Keywords: Dynamics; day-to-day; MFD; multi-modal; pricing

* Corresponding author. Tel.: +44(0)1413301839; E-mail address: wei.liu@glasgow.ac.uk (W. Liu)

1. Introduction

The notion of user equilibrium in transportation systems was first proposed by [Wardrop \(1952\)](#), and then extended by [Daganzo and Sheffi \(1977\)](#) (stochastic user equilibrium), and [Mahmassani and Chang \(1987\)](#) (bounded rational user equilibrium) and many other works. Considerable efforts in the literature have analyzed the equilibrium states when travelers have no incentive to switch mode, and/or departure time, and/or route, and have provided insightful ideas for both transportation planning and traffic management. However, in reality, it is often observed that traffic flows can fluctuate from time to time, due to the interference of external factors and change of the network itself (see, e.g., [Guo and Liu, 2011](#)). This raises the interests to analyze the day-to-day flow evolution in a transportation system with various models (for single-mode systems with either fixed or elastic demand, see, e.g., [Smith, 1984](#); [Friesz et al. 1994](#); [Cantarella and Cascetta, 1995](#); [Nagurney and Zhang, 1997](#); [Watling, 1999](#); [Watling and Hazelton, 2003](#); [Bie and Lo, 2010](#); [He and Liu, 2012](#); [Smith and Watling, 2016](#); [Xiao et al., 2016](#); and for multi-modal systems, see, e.g., [Cantarella et al., 2015](#); [Li and Yang, 2016](#)). Also, in recent years, more and more efforts have been dedicated to pricing or control strategies given that traffic pattern can change from day to day (e.g., [Sandholm, 2002](#); [Yang et al., 2007](#); [Smith and Mounce, 2011](#); [Ye and Yang, 2013](#); [Xiao and Lo, 2015](#); [Tan et al., 2015](#); [Ye et al., 2015](#); [Guo et al., 2015](#)).

However, most of the previous studies on the day-to-day flow evolution often simplify the traffic dynamics within a day, i.e., static traffic models are adopted to describe the traffic conditions within a day. This is often necessary to make these day-to-day models analytically tractable, but important features of the congestion patterns are missing. The traditional static network models (average travel cost/time vs. input demand level) are not always consistent with the physics and dynamics of traffic. It is known that the transportation networks are not memoryless, since the same inflow will create higher travel times in a more congested state, compared to an initially less congested (or uncongested) state. This is because for a given average flow (i.e. given demand rate over a period of time) the total cost (expressed in delay terms) depends on the initial state of the system (the initial level of congestion). Therefore, the estimated congestion toll based on idealized versions of these supply/performance curves (usually based on steady states) may not be optimal and accurate, and the system may be either still congested (if underpriced) or very uncongested (if overpriced) (see for example [Tsekeris and Geroliminis, 2013](#)).

A few studies have attempted to address the dynamic features of traffic under the day-to-day framework. [Ben-Akiva et al. \(1986\)](#) numerically analyzed the dynamic evolution process of departure rate in the single bottleneck (point-queue) model. Recently, [Guo et al. \(2017\)](#) made a solid effort to show the non-convergence of the conventional proportional swap system when

applied to the single bottleneck model with departure time choice. However, their analytical analysis, while insightful, relies on the simplified (within-day) traffic dynamics under the bottleneck model and ignores that real-time information could also affect travel choices in the context of within-day dynamics. Different from the above, the current study incorporates more realistic within-day traffic dynamics when considering travelers can adjust their mode choices from day to day, and traffic pattern (in a day) evolves over days. The complexity of the within-day dynamics generally leads to non-tractability (analytically) and no closed-form formulation. More importantly, besides travelers' day-to-day experience, real-time traffic condition (e.g., accessible through advanced traffic information platform, smartphone navigation apps) can affect travelers' choices, and thus will affect the day-to-day traffic evolution. This further complicates the dynamical system, which has been rarely modeled and explored in the literature.

To deal with the foreseen complexity of a model with many behavioral characteristics and degrees of freedom, we propose instead an aggregated traffic model. Specifically, we consider that the city network can be partitioned into two regions: the city center and the periphery (the extension to consider more regions is straightforward but more tedious).¹ A large-scale network traffic model expressed by the Macroscopic Fundamental Diagram (MFD) is adopted to capture the regional traffic dynamics (within a day) on the roadway network. The MFD of a network describes the relationships among network vehicle density, network average speed, and network space-mean flow (or travel production). This aggregated modeling approach enables and eases the dynamic modeling of large-scale transportation networks (for MFD-based modeling of multi-modal transportation system, see some initial attempts at [Geroliminis et al. \(2014\)](#); [Chiabaut \(2015\)](#) and others). The aggregated dynamic MFD model to capture the within-day dynamics is then integrated with (1) a discrete choice model to capture users' mode choices; (2) a day to day learning and evolution model to capture the variations of users' choices and traffic flows over calendar time; and (3) an adaptive aggregated pricing mechanism that affects travelers' mode choices and thus to improve system efficiency. The relevant assumptions regarding the coupled models are discussed in the following sections.

For the demand side, this study models two types of travel demands, i.e., traveling from periphery to city center and traveling within city center (trips from the city center to the periphery are neglected in this study). There are park-and-ride facilities located at the boundary of the city center, which has been implemented in many cities around the world, such as Munich, Stockholm, Amsterdam, and Glasgow. There are quite some studies looking into the park-and-ride problem with static traffic models, e.g., [Wang et al. \(2004\)](#); [Liu et al. \(2009\)](#); [Liu et al. \(2014\)](#); and [Pineda](#)

¹ Partitioning of a city network into multiple regions where each region exhibits a well-defined Macroscopic Fundamental Diagram (MFD) is discussed in, e.g., [Saeedmanesh and Geroliminis \(2016\)](#).

et al. (2016). For travelers living in the periphery, they can either drive to the city center, or take public transit, or drive to the park-and-ride facilities and then transfer to the public transit; while for travelers living in the city center, they can either drive or take public transit. For those who drive, they have to park their cars either at their final destinations or at the park-and-ride facilities.

Travelers can learn from both their travel experience and the real-time traffic information, and adjust their mode choices over time through a learning mechanism and consequently this influences the (within-day) dynamic traffic patterns in the city network (the day to day learning and evolution model). We assume that travelers have access to the real-time traffic information before starting their trips. In the literature, there is a branch of studies adopting “learning behavior” models (e.g., Horowitz, 1984; Watling, 1999; Bie and Lo, 2010) to capture people’s behavior in a day-to-day dynamical system. Specifically, travelers rely on their perceived travel cost (or utility/disutility) of different options to make decisions. Furthermore, the perceived travel cost is a convex combination of previous day’s perceived cost and experienced (or actual) cost. However, as one may tell, real-time information provision as well as its potential impacts are ignored in this type of learning models. Differently, we include the “predicted cost” (beyond past perceived and experience costs) in the learning model to capture how real-time (or nearly real-time) traffic condition might affect the choices of users and the traffic dynamics, where the “predicted cost” is based on the “current” (instantaneous at the departure time) traffic conditions. The incorporation of (real-time) dynamic conditions and the corresponding predicted cost into the day to day dynamical system becomes very relevant when flow-dependent within-day traffic dynamics are embedded into the day to day framework. In summary, this paper proposes a more general learning model where the perceived travel cost will not only depend on previous perceived and experienced travel costs, but also rely on the predicted costs (or cost estimates) based on real-time traffic conditions.

Moreover, to reduce traffic congestion and improve traffic efficiency in the city network, we propose an adaptive pricing strategy based on the transportation system state.² More specifically, we update pricing from period to period, where a period consists of a number of days (e.g., one period can be one month). Note that a period should be long enough such that: firstly at the end of each period, travelers’ mode choices and dynamic traffic pattern in the network will evolve to an equilibrium state from a day-to-day point of view (or at least close to that in practice); secondly, travelers will not get frustrated by frequently changing prices.³ In the end of a period,

² MFD-based parking pricing or congestion pricing has been considered in some recent studies, e.g., Zheng and Geroliminis (2016); Liu and Geroliminis (2016).

³ Roughly speaking, this is plausible in practice, and changing pricing strategy from day to day too frequently would be quite unlikely. Indeed, there is practice to update parking pricing from period to period (based on occupancy) in, e.g., San Francisco.

we can measure or observe the within-day traffic conditions at the equilibrium state (which might come from sensor data, loop detector data and GPS etc.). Based on these conditions, the transport manager or operator can update the parking pricing for the next period. Park-and-ride facilities at the boundary of the city center can provide a point of mode change (from driving to public transport) during travel. We would like to emphasize that the problem of our interest is not about computing the optimum solution for pricing based on the developed model, but a framework that can take advantage of observable system information. As one may see later in the formulations in Section 4, the proposed adaptive pricing mechanism only needs relatively aggregated traffic data that can be observed (e.g., the accumulation over time and some data to estimate the MFD of the regions), but does not need detailed information regarding travelers' behaviors (e.g., how the modal-split, travel cost, traffic dynamics equations exactly look like). This indicates that the adaptive mechanism is practical and flexible for implementation. In contrast, if we directly optimize the pricing, the underlying assumption is that we exactly know all the modelling details both about the formulations and the parameters.

The remainder is organized as follows. Section 2 firstly presents the city structure, the transport network, and the travel demand, and then formulates the within-day traffic dynamics. Day-to-day dynamics of the system and period-to-period adaptive pricing strategy are introduced and elaborated in Section 3. Then in Section 4, numerical experiments are conducted to illustrate the dynamic model (both within-day and day-to-day) and evaluate the efficiency of the proposed pricing strategy. Section 5 concludes the paper.

2. Model Formulation

In this section, firstly, we briefly describe the city, the multi-modal transport system, and the travel demand. We then present the within-day traffic dynamics in the road network.

2.1. The City, Transport, and Demand

We consider a concentric city, which is shown in Figure 1, and the geometric center is point O . We have the following assumption for the city representation.

Assumption 1. We adopt a one-dimensional representation of the city network, where locations with the same distance to the geometric center O are grouped as one unit (either as origin or destination). Each unit is then indexed by its distance x to the geometric center.

The one-dimensional representation of the city network is similar to those “linear monocentric city” models in the literature such as Verhoef (2005) or Wang et al. (2004). This representation tries to simulate the periphery-to-center traffic network. It can be readily extended to two dimensional models, i.e., we can index locations in the city with both x-coordinate and y-coordinate. In this case, the unit of the city corresponds to a point in the two-dimensional domain.

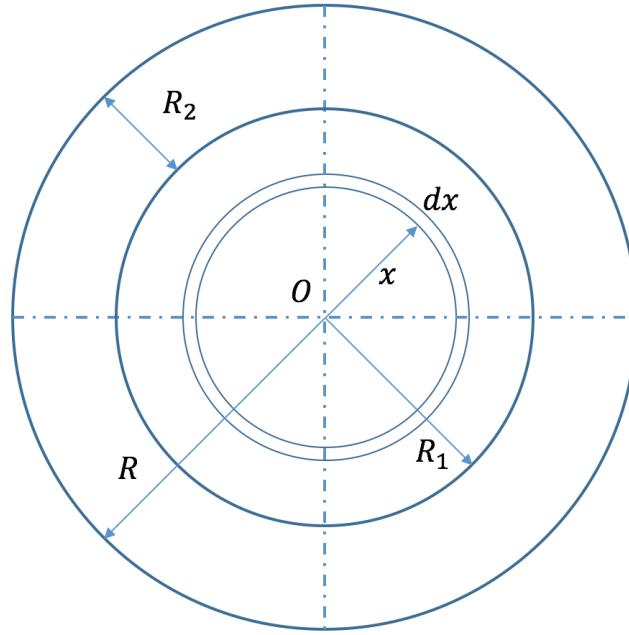


Figure 1. The concentric city structure

Assumption 2. The city is divided into two regions: the city center (or CBD, which is Region 1) and the periphery area (Region 2). For each region, the aggregated performance of the roadway network is described by a Macroscopic Fundamental Diagram (MFD).

As shown in Figure 1, the city center (Region 1) is the area from location 0 to R_1 , where location R_1 is the boundary of city center, and the area size is $A_1 = \pi R_1^2$. The periphery (Region 2) is the area from location R_1 to R , where $R = R_1 + R_2$, and location R is the boundary of the whole city, and the area size is $A_2 = \pi(R^2 - R_1^2)$. In this concentric city with two regions, total road length is TL_1 and TL_2 for Region 1 and Region 2 respectively. Generally, we expect that the road density in the city center would be higher than that in periphery (similar to Tsekeris and Geroliminis, 2013). Therefore, the total road length in the city center might be quite close to or even greater than that in periphery, although the area size might be much smaller.

As mentioned in the above, the Macroscopic Fundamental Diagram (MFD) is used to describe

the traffic dynamics in different regions. Specifically, for Region i , where $i \in \{1, 2\}$, the space-mean regional traveling speed depends on the regional traffic density, i.e., $v_i = v_i(k_i)$, where $k_i = n_i/TL_i$ is the car traffic density in the region, n_i is the traffic accumulation, and TL_i is the total road length. As TL_i is given, the speed function can also be simplified as $v_i = v_i(n_i)$. Given this regional speed-density relationship, it follows that the travel production is $P_i(n_i) = v_i(n_i) \cdot n_i$.

Assumption 3. Besides the roadway network, there are public transit services with dedicated right-of-way across the whole city.

Assumption 3 indicates that there is no direct flow interaction between private car traffic with the public transit. This consideration is to focus on the car network traffic dynamics and avoid further complexity in the multi-modal network. In case cars and public transit are interacting with each other in the roadway network, a three-dimensional fundamental diagram between car density, bus density and vehicle (or passenger) flow can be utilized, such as those in [Geroliminis et al. \(2014\)](#) or [Chiabaut et al. \(2014\)](#).

Assumption 4. Public transit service is known, where transit fare, frequency and speed are fixed and constant.

Specifically, in region i , public transit fare is f_i , transit frequency is λ_i , and transit speed is w_i .⁴ While we consider that the public transit service is given and known to us, future work might consider responsive public transit services such as those in [Zhang et al. \(2014\)](#), [Zhang et al. \(2016\)](#), and [Li and Yang \(2016\)](#). Note that $\lambda_1 \geq \lambda_2$ holds in this paper, as we consider that all public transit from Region 2 will also go through Region 1 (this is a minor assumption and can be relaxed readily). The operating cost of public transit per unit time in Region i is formulated as $\kappa_i(\lambda_i) \cdot A_i$.

Assumption 5. There are park-and-ride facilities located at the boundary of the city center, i.e., location R_1 .

⁴ Transit speed is the average speed after taking into account delays due to the pick-up and drop-off. Moreover, the transit speed in a region is assumed to be constant (note that we assume dedicated right-of-way for transit). Future study may consider a time-varying transit speed depending on the number of users carried. However, we expect that this would change the major results in this paper very little as we do not expect the transit speed to be extremely sensitive to the number of users (e.g., metro systems have relatively constant average speed, and in bus systems very often buses have limited allowed passengers). Similar assumptions are adopted in [Gonzales and Daganzo \(2012\)](#).

Those commuters choosing park-and-ride will park their cars at the boundary of the city center and then transfer to the public transit. For travelers driving to the city center, they will have to park at the city center. Parking fee at city center is p_1 , while parking fee is p_2 for park-and-ride facilities. Generally, one may expect a lower parking fee at the park-and-ride facilities (alternative forms of “lower parking fee” might be “discounted transit fare” for park-and-ride travelers in practice), while this is not relevant to our modeling framework.

Assumption 6. For a given origin-destination pair (x_o, x_d) and a given departure time t , total travel demand $\delta(x_o, x_d, t)$ is fixed and known.

Assumption 6 simply indicates that the (total) demand pattern over time is fixed and travelers cannot choose not-to-travel. Also, departure time choices are not considered. Specifically, the current study focuses on two types of origin-destination pairs, i.e., from Region 2 to Region 1, i.e., $x_o > R_1$ and $x_d \leq R_1$, and from Region 1 to Region 1, i.e., $x_o \leq R_1$ and $x_d \leq R_1$. These two types are the most typical ones, representing traveling to city center and traveling within city center respectively. However, we still have multiple origin-destination pairs as there are multiple origins (x_o) and destinations (x_d) in each region.

For commuters traveling from Region 2 to Region 1, there are three travel options: auto (private cars), public transit or park-and-ride (drive to the park-and-ride parking facilities and then transfer to transit). For commuters traveling within Region 1, they only have two travel modes: auto or transit. Later we will use a , b , p to represent modes of auto, public transit, and park-and-ride, respectively. Accordingly, travel demand choosing mode m is denoted by $\delta_m(x_o, x_d, t)$ where $m = \{a, b, p\}$ for $x_o > R_1$ and $m = \{a, b\}$ for $x_o \leq R_1$, and the feasible flow set is given in the following:

$$\Omega = \left\{ \mathbf{\delta} \geq 0 \mid \sum_m \delta_m(x_o, x_d, t) = \delta(x_o, x_d, t), \forall x_o, \forall x_d, \forall t \right\}, \quad (1)$$

where $\mathbf{\delta}$ is the vector for all $\delta_m(x_o, x_d, t)$ over different origin-destination pairs and departure times. The feasible flow set Ω is closed and convex.

Assumption 7. Trip length for travelers of a given origin-destination pair is denoted by $d(x_o, x_d)$, which is fixed and time-invariant.⁵

⁵ If one considers that travelers adapt route choices from day to day, this might not always hold. However, we expect the variation in trip length would be much less than that in trip time as it is less sensitive to congestion.

In reality, the trip length of travelers for specific origin-destination can be calibrated with real data. Generally, we expect that the trip length associated with the periphery traveling, i.e., from $x_o > R_1$ to city center boundary R_1 , is increasing with $x_o - R_1$, and the trip length associated with city center traveling, i.e., from $x_o \leq R_1$ to $x_d \leq R_1$, depends on $x_o - x_d$ and x_o and x_d . Later in Section 4, we will specify the trip distances for all origin-destination pairs.

2.2. Traffic Dynamics (within-day)

As we assume constant speed for the public transit, the modeling of transit traffic dynamics is straightforward and thus we omit the details. For auto and park-and-ride demand, as both of them involve the traffic flow in the road network, in the following we present the formulations governing the (within-day) dynamics. Similar dynamic equations have been presented in [Zheng and Geroliminis \(2013\)](#), [Ramezani et al. \(2015\)](#), but without origin-destination indexes x_o and x_d . Note that the boundary capacity is omitted from the equations.

The total accumulation in Region 1 or Region 2 at time t is the summation of all moving vehicles (with different origin-destination pairs) in the region at this time point, which is

$$n_1(t) = \int_0^{R_1} \int_0^R n_1(x_o, x_d, t) dx_o dx_d, \quad (2)$$

$$n_2(t) = \int_0^{R_1} \int_0^R n_2(x_o, x_d, t) dx_o dx_d + \int_0^{R_1} \int_{R_1}^{R_2} n_2^p(x_o, x_d, t) dx_o dx_d, \quad (3)$$

where $n_i(x_o, x_d, t)$ is the number of moving vehicles (auto mode) with origin-destination (x_o, x_d) in Region i at time t , and $n_2^p(x_o, x_d, t)$ is for those moving vehicles choosing park-and-ride mode.

We then can further determine the regional traveling speed at time t , i.e., $v_i(n_i(t))$, based on the regional speed-density relationship given in Subsection 2.1.

For auto travel demand from $x_o > R_1$ (Region 2) to $x_d \leq R_1$ (Region 1), they firstly travel through Region 2 and then enter Region 1. The conservation of flows (over clock time) in Region 2 requires that

$$\frac{dn_2(x_o, x_d, t)}{dt} = \delta_a(x_o, x_d, t) - o_2(x_o, x_d, t), \quad (4)$$

where $n_2(x_o, x_d, t)$ and $o_2(x_o, x_d, t)$ are the accumulation and outflow (in Region 2) of traffic from x_o to x_d departing at time t . Eq.(4) simply says that the change of accumulation (in Region 2) of traffic from x_o to x_d is equal to the inflow (equals the demand) minus the outflow (equals

arrival rate to Region 1). The total travel production of region i is $P_i(n_i(t)) = v_i(n_i(t)) \cdot n_i(t)$ at time t , which is indeed the integral of all $n_i(x_o, x_d, t)$ pairs across all x_o and x_d multiplied by $v_i(n_i(t))$. As the regional speed is assumed to be common for all users, we can approximate the demand specific outflow as the following:

$$o_2(x_o, x_d, t) = \frac{n_2(x_o, x_d, t) \cdot v_2(n_2(t))}{d(x_o, R_1)}, \quad (5)$$

where $d(x_o, R_1)$ is the trip length in Region 2 of these vehicles, and $v_2(n_2(t))$ is the Region 2 speed at time t . Eq.(5) assumes that there is always a direct relationship between production (as expressed by the product of accumulation and speed) and outflow, while the trip length is time-invariant. The assumption of a low-scatter regional outflow MFD is based on the equivalent assumption of a time-invariant regional trip length. Although there are empirical verifications about the validity of this model with aggregated data (e.g., [Geroliminis and Daganzo, 2008](#)), it should not be considered as a universal law. For example, strong fluctuations in the demand that create fast evolving transients can influence the trip length distribution in a region at a specific time, potentially causing the ratio of production over trip length approximation of outflow to have inaccuracies. While this is a valid assumption for a range of cases, further research would be useful to study under what conditions more complex formulations of dynamics (with delays) are required. Some recent efforts in this direction can be found in [Lamotte and Geroliminis \(2016\)](#), [Mariotte et al. \(2017\)](#), while the first who proposed a trip-based accumulation model is [Arnott \(2013\)](#).

Furthermore, after these vehicles (from $x_o > R_1$ to $x_d \leq R_1$) entering into Region 1, similarly the accumulation (in Region 1) and outflow (arrival to destination x_d) over (clock) time satisfy the following dynamic relations.

$$\frac{dn_1(x_o, x_d, t)}{dt} = o_2(x_o, x_d, t) - o_1(x_o, x_d, t), \quad (6)$$

$$o_1(x_o, x_d, t) = \frac{n_1(x_o, x_d, t) \cdot v_1(n_1(t))}{d(R_1, x_d)}, \quad (7)$$

where $n_1(x_o, x_d, t)$ and $o_1(x_o, x_d, t)$ are the accumulation and outflow (in Region 1) of traffic from x_o to x_d departing at time t , $d(R_1, x_d)$ is trip length of these vehicles in Region 1. Note that, in Eq.(6), the inflow of these vehicles in Region 1 is equal to the outflow from Region 2.

For park-and-ride demand, when they are traveling in Region 2, the accumulation and outflow also satisfy similar conditions as follows.

$$\frac{dn_2^p(x_o, x_d, t)}{dt} = \delta_p(x_o, x_d, t) - o_2^p(x_o, x_d, t). \quad (8)$$

$$o_2^p(x_o, x_d, t) = \frac{n_2^p(x_o, x_d, t) \cdot v_2(n_2(t))}{d(x_o, R_1)}. \quad (9)$$

As these park-and-ride travelers transfer to public transit and do not drive to Region 1, therefore $n_1^p(x_o, x_d, t) = 0$ and $o_1^p(x_o, x_d, t) = 0$. And the driving distance for park-and-ride travelers is $d(x_o, R_1)$. We can also write down the dynamic equations for traffic from $x_o \leq R_1$ to $x_d \leq R_1$ (traveling within the city center) in a similar way. Note that when these equations are applied in the day to day framework, an additional index for days q have to be used (as we will see in Section 3.1), which is not included here for simplicity.

3. Day-to-day Dynamics and Adaptive Pricing

In this section, firstly, we present the day-to-day learning process of travelers (learn from both previous experience and prediction based on real-time traffic conditions), and then illustrate the period-to-period adaptive pricing strategy to reduce congestion and total social cost.

3.1. Day-to-day Dynamics with Learning Behavior

Consider a discrete-time day-to-day evolution model with a learning process where the calendar time is denoted by q , and the time step is $\Delta q = 1$, i.e., one day. Travelers are assumed to make choices based on their perceived utilities of different modes. Furthermore, the perceptions are updated from day to day which takes into account the experienced conditions (from the previous day's experience) and the current traffic conditions at the departure time (from, e.g., traveler information system) by certain rules, which are presented in the following.

For travelers from x_o to x_d and with a departure time of t , let $c_m^{p,q}(x_o, x_d, t)$ be the perceived travel cost of mode m on day q , and let $c_m^{e,q}(x_o, x_d, t)$ be the experienced travel cost of mode m on day q , and let $c_m^q(x_o, x_d, t)$ be the predicted travel cost of mode m based on (real-time)

instantaneous traffic conditions (at time t)⁶ on day q , e.g., through a real-time information system. The perceived travel cost of travel mode m at day $q+1$ is determined according to the following:

$$\begin{aligned}
c_m^{p,q+1}(x_o, x_d, t) = & \\
& \omega \cdot c_m^{p,q}(x_o, x_d, t) + (1 - \omega) \cdot c_m^{e,q}(x_o, x_d, t). \\
& + \rho \cdot (c_m^{q+1}(x_o, x_d, t) - c_m^q(x_o, x_d, t))
\end{aligned} \tag{10}$$

where $m = \{a, b, p\}$ for $x_o > R_1$ and $m = \{a, b\}$ for $x_o \leq R_1$. In Eq.(10), $0 < \omega < 1$ is a learning parameter associated with the previous day's perception and experience ("learning factor"), and $\rho \geq 0$ is a parameter associated with the current and previous day's predictions based on instantaneous (current) traffic conditions at the same departure time ("information factor"). Eq.(10) is a generalization of most existing "learning behavior" models (e.g., [Bie and Lo, 2010](#)) where $\rho = 0$ and the perception is only a linear combination of previous perception and experience.

In Eq.(10), a larger learning factor ω means that the travelers put more weight on yesterday's perceived cost (comes from long-term experience) and less on yesterday's experienced cost when updating perception, indicating less sensitivity to a single day's experience (as shown later in numerical experiments, over-sensitivity to single day experience might lead to non-convergence of the day to day evolution model).

Furthermore, $\rho > 0$ means that travelers take into account real-time traffic information (as the updating of perceived cost takes into account the predicted cost based on current traffic conditions). Particularly, we consider that travelers compare the current traffic conditions with the ones received from the previous day, and evaluate whether the situation today (of different modes) is worse or better. For instance, $c_a^{q+1}(x_o, x_d, t) - c_a^q(x_o, x_d, t) > 0$ suggests that the travel cost estimate based on the current traffic condition on day $q+1$ is worse than that on the previous day, which leads to a larger perceived cost on day $q+1$, i.e., a larger $c_a^{p,q+1}(x_o, x_d, t)$. The magnitude of ρ can reflect the relative sensitivity of travelers to the real-time traffic conditions. A very large ρ means that traveler will be affected significantly by information on traffic conditions, while $\rho \rightarrow 0$ means that travelers are not influenced by real-time conditions at all (or do not have access to). This modeling framework offers us a way to model and evaluate

⁶ This instantaneous traffic conditions at departure time later might be quite often referred to as "current condition". Moreover, the cost based on instantaneous traffic conditions will be termed as predicted cost based on "current condition" later.

how real-time information provision and dynamic traffic conditions might affect travelers' choices, and thus change the system dynamics (both within-day and day-to-day). To the best of our knowledge most commercial real-time traffic information platforms provide instantaneous travel time information. However, if different types of predictions (rather than the one based on current traffic conditions) are available, it can be readily accommodated in Eq.(10).

The travelers choose their travel modes according to the perceived utilities of different modes. The perceived utility of mode m on the day q can be defined as:

$$U_m^{p,q} = -\left[c_m^{p,q}(x_o, x_d, t) + cf_m(x_o, x_d) \right] + \varepsilon_{m,t}. \quad (11)$$

The random terms $\varepsilon_{m,t}$ are assumed identically and independently distributed with a Gumbel probability distribution function with mean zero, and variance $\frac{1}{6}\pi^2\theta$, where θ is a constant parameter to be estimated for real applications. $cf_m(x_o, x_d)$ is a commonality factor of mode m between origin x_o and destination x_d to account for the overlaps (as well as correlations) between different modes (assumed be to time-invariant). Then for travelers from location x_o to x_d at departure time t , on day q the proportion choosing mode m can be given by a logit formula as follows

$$\Pr_m^q(x_o, x_d, t) = \frac{\exp\left(-\theta \cdot \left(c_m^{p,q}(x_o, x_d, t) + cf_m(x_o, x_d)\right)\right)}{\sum_j \exp\left(-\theta \cdot \left(c_j^{p,q}(x_o, x_d, t) + cf_j(x_o, x_d)\right)\right)}. \quad (12)$$

where $m, j \in \{a, b, p\}$ for $x_o > R_1$, and $m, j \in \{a, b\}$ for $x_o \leq R_1$.

Incorporating a commonality factor $cf_m(x_o, x_d)$ into the logit mode is termed as C-logit in the literature, which is to account for overlaps between routes (in this paper for modes). As park-and-ride is a mixed travel mode which associates two single modes: auto and transit, this choice probability formulation helps to capture the overlaps between park-and-ride modes with other modes. Note that if there is no overlap between modes (or routes), the commonality factor $cf_m(x_o, x_d)$ will be zero, and Eq.(12) reduces to the standard multi-nominal logit model. [Cascetta et al. \(1996\)](#) proposed several function forms for the commonality factor in Eq.(12). In this article, we follow [Zhou et al. \(2012\)](#), and adopt the following form:

$$cf_m(x_o, x_d) = \beta \cdot \ln \left(\sum_j \left(\frac{L_{jm}}{\sqrt{L_j} \cdot \sqrt{L_m}} \right) \right), \quad (13)$$

where β is a model parameter to be calibrated for real applications, L_{jm} is the trip length common to mode j and mode m , L_j and L_m is the trip length of mode j and m . In the current study, for travelers from $x_o > R_1$, park-and-ride mode overlaps with auto mode for trip length $d(x_o, R_1)$, and overlaps with transit mode for trip length $d(R_1, x_d)$. Based on Eq.(12), the demand for mode m for given origin-destination pair and departure time is

$$\delta_m^q(x_o, x_d, t) = \text{Pr}_m^q(x_o, x_d, t) \cdot \delta(x_o, x_d, t). \quad (14)$$

Note that $\sum_m \text{Pr}_m^q(x_o, x_d, t) = 1$ and $\sum_m \delta_m^q(x_o, x_d, t) = \delta(x_o, x_d, t)$, and the day index q is added to the notations for demand of different modes.

The above dynamical system can be written in the following vector-matrix form

$$\begin{aligned} \mathbf{c}^{p,q+1} &= \omega \cdot \mathbf{c}^{p,q} + (1-\omega) \cdot \mathbf{c}^{e,q} + \rho \cdot (\mathbf{c}^{q+1} - \mathbf{c}^q) \\ \boldsymbol{\delta}^{q+1} &= \mathbf{D} \cdot \text{Pr}(\mathbf{c}^{p,q+1}) \end{aligned}, \quad (15)$$

where \mathbf{c}^p , \mathbf{c}^e and \mathbf{c} are the perceived cost, experienced cost and predicted cost vectors, and \mathbf{D} is a diagonal matrix which has demand $\delta(x_o, x_d, t)$ as its diagonal elements, and $\text{Pr}(\cdot)$ is the C-logit choice model. As the experienced costs and predicted costs are both based on the realized flows, i.e., $\mathbf{c}^{e,q+1} = c^e(\boldsymbol{\delta}^{q+1})$, $\mathbf{c}^q = c(\boldsymbol{\delta}^q)$, and $\mathbf{c}^{q+1} = c(\boldsymbol{\delta}^{q+1})$, Eq.(15) can be rearranged as

$$\begin{aligned} \mathbf{c}^{p,q+1} &= \omega \cdot \mathbf{c}^{p,q} + (1-\omega) \cdot c^e(\boldsymbol{\delta}^q) + \rho \cdot (c(\boldsymbol{\delta}^{q+1}) - c(\boldsymbol{\delta}^q)) \\ \boldsymbol{\delta}^{q+1} &= \mathbf{D} \cdot \text{Pr}(\mathbf{c}^{p,q+1}) \end{aligned}. \quad (16)$$

Using the vector of perceived costs as the state identifier, the fixed point of the above system can then be derived as

$$\mathbf{c}^{p,*} = c^e(\mathbf{D} \cdot \text{Pr}(\mathbf{c}^{p,*})). \quad (17)$$

This is indeed the C-logit based user equilibrium condition, of which we omit the detailed discussions. Note that while $\rho \cdot (c(\boldsymbol{\delta}^{q+1}) - c(\boldsymbol{\delta}^q))$ is added to the dynamical system defined in Eq.(16) compared to the existing literature to account for real-time information's impact (e.g., [Bie and Lo, 2010](#); [Watling, 1999](#)), at the fixed point we should have $\rho \cdot (c(\boldsymbol{\delta}^{q+1}) - c(\boldsymbol{\delta}^q)) \rightarrow 0$ since $\boldsymbol{\delta}^{q+1} \rightarrow \boldsymbol{\delta}^q \rightarrow \boldsymbol{\delta}^*$. This means that the fixed points of the dynamical system in the above will be identical to those under $\rho = 0$.

We notice that $c(\boldsymbol{\delta}^q) = c^e(\boldsymbol{\delta}^q)$ generally does not hold. This is because that cost estimates based on real-time information usually differs from the experienced costs. Certain interdependent

relationships exist between them, and indeed a vast literature in the travel time estimations indicates that discrepancy between the experienced time and the instantaneous estimation of travel time for smoothly varying traffic conditions might be in the range of 5-10%, see, e.g., [Yildirimoglu and Geroliminis \(2013\)](#). Furthermore, the complexities of the simulation-based functions $c^e(\cdot)$ and $c(\cdot)$ given in Eq.(16) limit the analytical tractability of the dynamical system described in the above. These complexities are mainly due to the non-closed-form and asymmetric modeling of within-day traffic congestion, and the non-closed-form modeling of real-time information. We leave these very interesting but challenging issues for future research, and in this study explore the evolution process based on the proposal dynamical model via extensive numerical experiments.

3.2. Experienced Cost and Predicted Cost

As described in Eq.(10), the travelers update their perceived cost based on experienced cost and predicted cost (or cost estimate). The experienced travel cost contains both monetary cost and time cost, which is given in the following. Note that later when we discuss the period-to-period adaptive pricing strategy where each period contains a number of days, the parking price might be different on different periods. We denote the period by η , and suppose that day q belongs to period η . Then, on day q , for a traveler traveling from origin x_o in Region 2 to destination x_d in Region 1 and departing from home at time t , experienced auto travel cost would be

$$c_a^{e,q}(x_o, x_d, t) = \alpha \cdot \left(\frac{d(x_o, R_1)}{\bar{v}_2^q(t)} + \frac{d(R_1, x_d)}{\bar{v}_1^q(t)} \right) + p_1^\eta, \quad (18)$$

where $\bar{v}_i^q(t)$ is the experienced average speed for the traveler in region i , α is the value of unit travel time, and p_1^η is the parking fee in the city center (region 1) at period η . Note that the exact speed during the trip can change over (clock) time, and $\bar{v}_i^q(t)$ is the average value associates with the experienced trip time and distance (to be discussed later), which can be obtained after solving the experienced travel time in Eq.(21). Similarly, the experienced travel cost by taking public transit can be given as

$$c_t^{e,q}(x_o, x_d, t) = \alpha \cdot \left(\frac{1}{2\lambda_2} + \frac{d(x_o, R_1)}{w_2} + \frac{d(R_1, x_d)}{w_1} \right) + f_2, \quad (19)$$

where $1/2\lambda_2$ is an approximation of the waiting time for public transit, f_2 is the transit fare, and w_i is the transit speed in Region i where $i \in \{1, 2\}$. Note that the transit service frequency, speed, and fare are considered to be time-invariant. For park-and-ride mode, travel cost is

$$c_p^{e,q}(x_o, x_d, t) = \alpha \cdot \left(\frac{d(x_o, R_1)}{\bar{v}_2^q(t)} + t_r + \frac{1}{2\lambda_1} + \frac{d(R_1, x_d)}{w_1} \right) + p_2^\eta + f_1. \quad (20)$$

By using park-and-ride in the city boundary, besides the driving time (from home to the park-and-ride facilities), transit waiting time, and in-vehicle transit time, the travelers have to spend a transfer time t_r , which usually will depend on the number of park-and-ride facilities accessible at the city center boundary and distance of the parking facility to the public transit. In this paper, we simply adopt a constant value for t_r . Also, the cost of park-and-ride mode includes a fee of p_2^η for parking at the park-and-ride facility (for period η), and a transit fare f_1 for taking transit from the boundary of city center to the final destination. Generally, in reality we can expect that parking fee p_2^η at the park-and-ride is less than parking fee p_1^η in the city center.

Experienced travel costs of commuters from Region 1 to Region 1 (or within the city center) by taking auto, transit can be determined similarly. However, there is no park-and-ride option for commuters traveling within the city center. The current paper models the large-scale city network in a relatively aggregated manner, and does not consider minor (while possible) unfavorable situations associated with park-and-ride such as travelers who live within the city center but close to the city center boundary might choose park-and-ride to enjoy the much lower parking fee (or discounted transit fare).

Now we turn to describe the determination of experienced travel cost (we omit the day index q here). To obtain the experienced travel costs, we need to obtain the experienced travel time first. The transit travel time is straightforward as we assume constant transit speed. For auto mode, the experienced travel time can be obtained by numerically solving

$$d(x_o, x_d) = \int_t^{t+T(x_o, x_d, t)} v^e(w) dw. \quad (21)$$

where $T(x_o, x_d, t)$ is the experienced travel time for auto commuters from x_o to x_d and departing at time t , and $v^e(\cdot)$ is the experienced speed over time (this will be known to us after “it becomes an experience”). Note that, when the traveling occurs in Region i , $v^e(\cdot)$ should be the speed in Region i , where $i \in \{1, 2\}$. Similarly, we can compute the experienced driving time of a traveler choosing park-and-ride mode. With the experienced travel time in Eq.(21), we then can compute experienced travel cost, as well as the average experienced speed. We also would like to mention here that later in the simulation, the time horizon (in a day) has been discretized into identical intervals with a length of δt . In order to have an accurate and consistent calculation of experienced travel time $T(x_o, x_d, t)$ under the discretized numerical setting, we should allow

$T(x_o, x_d, t)$ to be a non-integer times of the unit time interval δt . Therefore, we have

$$T(x_o, x_d, t) = (\tau + \phi) \cdot \delta t. \quad (22)$$

where τ is an integer and ϕ is a non-integer (unless it equals zero) and $0 \leq \phi < 1$. These two values can be uniquely determined as follows

$$d(x_o, x_d) = \sum_{w=t}^{t+\tau-1} v^e(w) \cdot \delta t + \phi \cdot v^e(t + \tau) \cdot \delta t, \quad (23)$$

where $\sum_{w=t}^{t+\tau-1} v^e(w) \cdot \delta t \leq d(x_o, x_d) < \sum_{w=t}^{t+\tau} v^e(w) \cdot \delta t$ and $0 \leq \phi < 1$. Note that in Eq.(22) and Eq.(23) we still keep the same notation t for the clock time though it has been discretized.

To obtain the predicted travel costs (or cost estimates) based on instantaneous conditions (“current condition” at the departure time), we just need to replace the average speed (over time during the trip) in travel cost formulations in Eq.(18) and Eq.(20) with the instantaneous speed at the departure time. The predicted cost (usually travel time) can come from, existing navigation services. It is worth mentioning that the formulation of predicted travel costs in this paper do not cover all possible types of predictions in practice. However, different types of predictions can be similarly incorporated into Eq.(10).

3.3. The dynamic user equilibrium

We now briefly describe the dynamic user equilibrium in the network (which is expected to be achieved at the end of the traffic evolution process). As we discuss the user equilibrium state, the day index q is omitted. For presentation and illustration purpose, we add the flow vector δ (which is given in Eq.(1)) into the experienced cost function given in Section 3.2, and then the dynamic user equilibrium flow pattern δ^* solves the following infinite-dimensional variational inequality problem,

$$\int_t \int_0^R \int_0^R \sum_m c_m^e(x_o, x_d, t, \delta^*) \cdot [\delta_m(x_o, x_d, t) - \delta_m^*(x_o, x_d, t)] \cdot dx_o \cdot dx_d \cdot dt \geq 0, \quad (24)$$

subject to the flow conservation, flow dynamics, cost formulations, and modal-split defined in Section 2 and Section 3. It can be shown that the solution to Eq.(24) will satisfy the conditions in Eq.(17) for the fixed point of the system.

Firstly, the feasible flow set Ω for δ given in Eq.(1), by construction, is closed and convex. Secondly, the within-day traffic dynamics formulations in Section 2 are continuous functions, and experienced travel cost formulations in Section 3 are continuous combinations of time cost and monetary cost. Therefore, the experienced cost $c_m^e(x_o, x_d, w, \delta)$ given in Eq.(24) is expected

to be continuous over δ . According to, e.g., [Smith and Wisten \(1995\)](#), the existence of the dynamic user equilibrium is expected (one may also refer to Schauder's fixed-point theorem). The uniqueness of the dynamic user equilibrium generally requires that $c_m^e(x_o, x_d, w, \delta)$ is strongly monotonic over δ ([Nagurney, 1993](#)), which does not generally hold in this paper, although we expect that they are monotonic. We leave such questions for future research while we in this study focus on the integration of impacts of real-time information on travelers' choices in a day to day evolution context.

3.4. System Performance and Period-to-period Adaptive Pricing

We now discuss an adaptive pricing strategy (from period-to-period) to reduce the congestion and the total social cost. In particular, the total social cost can be reduced by appropriately adjusting the parking prices p_1 and p_2 . As one will see shortly, the proposed adaptive strategy takes advantage of post-experience measurements or observations of the system conditions (in practice, this will rely on data from sensors, loop detectors, GPS etc.), but does not need detailed information regarding users' learning behavior, modal-split, cost/utility formulations, which can be regarded as a practical way for pricing implementation.

Specifically, the adaptive pricing strategy tries to drive the urban network to operate at the critical accumulation (with the maximum production). Operation at the maximum production for the network is generally beneficial, which has been discussed in many previous studies (e.g., [Gonzales and Daganzo, 2012](#); [Liu and Geroliminis, 2016](#)). However, if alternative target is set, Eq.(25) (price adjustment function presented later) can be modified accordingly to meet the target.⁷

We present the detailed formulation regarding the adaptive pricing now. As mentioned, a period is denoted by η , and the length of a period is $\Delta\eta$, which can be, e.g., one month. Parking pricing in Region i (price in Region 2 is for park-and-ride facilities) in the period η is p_i^η . After we implement the prices in the beginning of period η , the traffic pattern in a day (including modal-split, dynamic traffic pattern on the road network) will evolve from day to day (the evolution dynamics over calendar time are modeled in Section 3.1), and approach an equilibrium state in the end of this period (or at least close to an equilibrium state, this usually requires the length of the period to be long enough). These equilibrium traffic conditions on the last day of period η

⁷ For multi-region cities, operation around the maximum production for all regions is often a nearly optimal solution, but is easy for implementation and verification in practice. More complex control strategies to coordinate different regions might have to be introduced (see, e.g., [Ramezani et al. 2015](#)) to achieve a minimum delay objective.

can be observed or measured, which give us, e.g., regional accumulation and speed profiles (for all regions) over (clock) time, i.e., we will know the accumulation profile $n_1^\eta(t)$ and $n_2^\eta(t)$ over the modeling duration. Note that these are aggregated variables, which are easy to measure with current sensor and GPS technologies.

Parking pricing in Region i in period $\eta+1$ is then updated by the following

$$\begin{aligned}
p_i^{\eta+1} = & p_i^\eta \\
& + p_{i,0} \cdot \int_{t_s}^{t_e} \max\{0, n_i^\eta(w) - n_i^{cri}\} dw \quad , \\
& - p_{i,0} \cdot \int_{t_s}^{t_e} \max\left\{0, n_i^{cri} - \max_{t \in [t_s, t_e]} \{n_i^\eta(t)\}\right\} dw
\end{aligned} \tag{25}$$

where $n_i^{cri} = k_i^c \cdot TL_i$ is the critical accumulation of Region i beyond which the regional travel production decreases with accumulation, and $n_i^\eta(t)$ for $t \in [t_s, t_e]$ is observed at the end of period η , and $p_{i,0}$ is a coefficient for adjusting the parking price. These coefficients should be appropriately chosen in practice to avoid big fluctuation (i.e., a too big coefficient) and to avoid non-effective price update (i.e., a too small coefficient).⁸ Simply speaking, the second term in Eq.(25) tries to eliminate time durations with congested conditions, i.e., when $n_i^\eta(t) > n_i^{cri}$, while the third term tries to avoid overpricing and underutilization of network capacity.

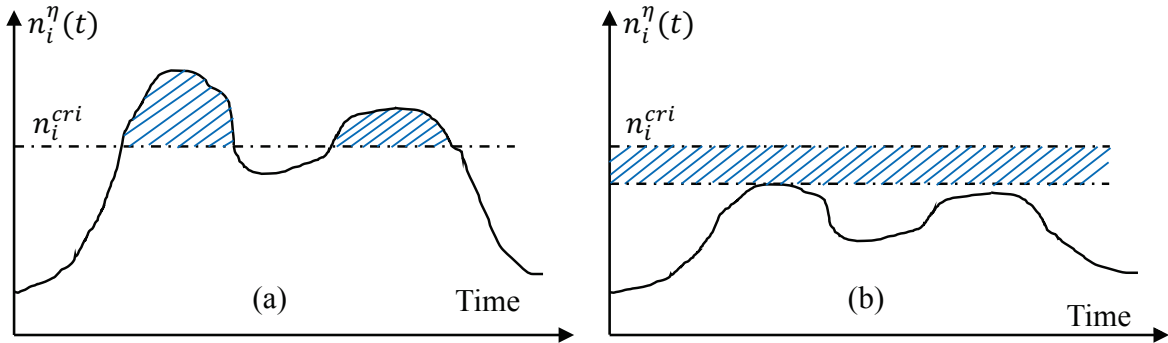


Figure 2. Graphical explanation of second and third terms in the right-hand side of Eq.(25)

More specifically, in Eq.(25), one can see that the price in the new period will be based on the last price (first term in right-hand side), and the additional congestion delays (the second term in

⁸ This paper considers constant pricing for parking, i.e., the parking fees are time-independent for the modeling period (usually the congested period), which can be readily extended to time-dependent parking pricing. Specifically, we can divide the time horizon into multiple intervals, and assume different parking fee rate (dollars per unit time) for different time intervals. In the price adjustment function in Eq.(25), we then adjust the pricing rate. However, instead of using accumulation profile for the whole modeling duration to calculate the price adjustment in Eq.(25), we should use the accumulation profile for a specific time interval to update the pricing rate for this time interval.

right-hand side) and the wasted roadway capacity (third term in right-hand side). The second term is proportional to the total additional congestion delays when regional accumulation goes beyond the critical value, which is the shadow area displayed in Figure 2(a). If the accumulation never exceeds the critical value n_i^{cri} , the second term will be zero, and the third term then will be strictly positive. The third term has not an exact physical meaning compared with the second term, but can be regarded as the total number of additional traffic (accumulated over time) that can be put into the roadway network without causing accumulation to go beyond critical values and additional congestion delay, which is the shadow area displayed in Figure 2(b). Lastly, we would like to point out that if the above adaptive pricing converges, it means that both areas in Figure 2(a) and Figure 2(b) approach zero, suggesting no additional congestion delay and no systematical waste of roadway capacity (i.e., at least for some durations, the region accumulation will reach the critical value).

There are multiple system efficiency measures of our interest when implementing the adaptive pricing scheme. The total travel cost of travelers on day q , which includes the fees or fares paid by the travelers, is

$$TC^q = \int_{t_s}^{t_e} \int_0^{R_1} \int_0^R \left(\sum_{m \in \{a,t,p\}} \delta_m^q(x_o, x_d, t) \cdot c_m^{e,q}(x_o, x_d, t) \right) dx_o dx_d dt + \int_{t_s}^{t_e} \int_0^{R_1} \int_0^{R_1} \left(\sum_{m \in \{a,t\}} \delta_m^q(x_o, x_d, t) \cdot c_m^{e,q}(x_o, x_d, t) \right) dx_o dx_d dt \quad (26)$$

where t_s is the start time (clock time) and t_e is the end time (clock time) for the modeling duration (within-day). In Eq.(26), the first and second term are the total costs of travelers from Region 2 and Region 1, respectively. The operating cost of public transit service covering the whole city is

$$K^q = \int_{t_s}^{t_e} (\kappa_1(\lambda_1) \cdot A_1 + \kappa_2(\lambda_2) \cdot A_2) dt. \quad (27)$$

The total transit revenue (fares collected) is

$$R_t^q = \int_{t_s}^{t_e} \int_0^{R_1} \int_0^R \left(\delta_t^q(x_o, x_d, t) \cdot f_2 + \delta_p^q(x_o, x_d, t) \cdot f_1 \right) dx_o dx_d dt + \int_{t_s}^{t_e} \int_0^{R_1} \int_0^{R_1} \left(\delta_t^q(x_o, x_d, t) \cdot f_1 \right) dx_o dx_d dt \quad (28)$$

Similar to the total travel cost, in Eq.(28), the first term and second term are the total transit fares collected from travelers from Region 2 and Region 1, respectively. Note that in the first term, transit fares are different for travelers (from Region 2) choosing transit mode and park-and-ride mode. Specifically, transit fare within center zone f_1 generally would be no great than f_2 as distance covered by transit is shorter. Furthermore, the total parking fee revenue is

$$\begin{aligned}
R_p^q &= \int_{t_s}^{t_e} \int_0^{R_1} \int_{R_1}^R (\delta_a^q(x_o, x_d, t) \cdot p_1^n + \delta_p^q(x_o, x_d, t) \cdot p_2^n) dx_o dx_d dt \\
&+ \int_{t_s}^{t_e} \int_0^{R_1} \int_0^{R_1} (\delta_p^q(x_o, x_d, t) \cdot p_1^n) dx_o dx_d dt
\end{aligned} \tag{29}$$

Note again that day q should be within period η . Similarly, in Eq.(29), the first term and second term are the total parking fees collected from travelers from Region 2 and Region 1, respectively. Those choosing park-and-ride pay a different parking fee from those driving to the city center. With Eq.(26), Eq.(27), Eq.(28) and Eq.(29), the total social cost on day q can be written as:

$$TSC^q = TC^q + K^q - R_t^q - R_p^q. \tag{30}$$

The transit revenue and parking fee are not considered as parts of the social cost.

4. Numerical experiments

This section presents some numerical experiments to illustrate and verify the dynamical model and analysis in the paper. We firstly list the major numerical settings, and then discuss the day-to-day dynamical model and evolution, and period-to-period adaptive pricing, respectively.

4.1. Numerical Setting

While the analytical model assumes the (clock) time and the space (location) to be continuous, for numerical analysis, the time horizon (within a day) is discretized into multiple small time intervals (five minutes per interval, which is consistent with the discretization for MFD dynamics in the literature), and the city is discretized into multiple small space intervals (500 meters per interval). Origins and destinations are indexed based on the space interval. For instance, O-D pair (10, 2) means origin is the tenth space interval, i.e., location from 4.5 km to 5.0 km; and destination is the second space interval, i.e., location from 0.5 km to 1.0 km. We now list other major numerical settings in Tables 1- 4.

Table 1. Numerical setting for the city

<i>The city</i>	<i>Specification</i>
The city center boundary location	$R_1 = 3$ (km)
The area size of city center	$A_1 = 28.27$ (km ²) $\equiv \pi(R_1)^2$
The city boundary location	$R = 6$ (km); then $R_2 = 3$ (km)
The area size of periphery	$A_2 = 84.82$ (km ²) $\equiv \pi(R)^2 - \pi(R_1)^2$;
Total road length in city center	$TL_1 = 100$ (km);
Total road length in periphery	$TL_2 = 120$ (km);

Table 2. Numerical setting for the MFDs of regions in the city

<i>Aggregated Traffic Model</i>	<i>Specification</i>
Speed function	$v_i(k_i) = v_i^0 \cdot e^{-v_i^1 \cdot k_i}$ for $k_i \geq k_i^c$; $v_i(k_i) = v_i(k_i^c)$ for $k_i < k_i^c$
Parameters for Region 1	$v_1^0 = 68$ (km/h), $v_1^1 = 5.4 \times 10^{-2}$, $k_1^c = 20$ (veh/km);
Parameters for Region 2	$v_2^0 = 108.7$ (km/h), $v_2^1 = 5.4 \times 10^{-2}$, $k_2^c = 20$ (veh/km);

Given the regional road length and speed-density relationship specified in the above, the regional production-accumulation relationship for both regions can be determined as well based on Subsection 2.1. While we omit the details, we highlight here that the periphery generally has a “larger” production-accumulation curve due to its longer road length and higher free-flow speed.

Table 3. Numerical setting for the public transit and park-and-ride services in the city

<i>Public service parameters</i>	<i>Specification</i>
Transit fees	$f_1 = 3$ (EUR); $f_2 = 4$ (EUR)
Transit frequencies	$\lambda_1 = 10$ (veh/h); $\lambda_2 = 8$ (veh/h)
Transit speeds	$w_1 = 20$ (km/h); $w_2 = 30$ (km/h)
Park-and-ride transfer time	$t_{tr} = 6$ (min/trip);

Table 4. Characteristics related to the population⁹:

<i>Factors</i>	<i>Specification</i>
Learning factor	$\omega = 0.70$;
Information factor	$\rho = 1.0$;
Coefficient in logit model	$\theta = 0.15$;
Coefficient in commonality factor	$\beta = 1.0$;

Now we turn to the travel demand profile (which is assumed to be identical for every day, but note that later in Section 4.3 we will examine the case where demand uncertainty exists). The aggregated demand over time is described in Figure 3(a), where the whole modeling duration is equal to four hours (i.e., $t_s = 0$ and $t_e = 4$) with a high demand duration of around 2 hours, which simulates the peak durations. Note that while the aggregated demand from Region 2 is higher, but they all travel to Region 1, thus Region 1 (city center) is still the most congested part of the city (this is often the case in reality). Figure 3(b) further displays the demand distribution with respect to origins and destinations. As can be seen, all travel demand goes to Region 1 (blue dash-dot line), and more travelers are from Region 2 (black solid line).

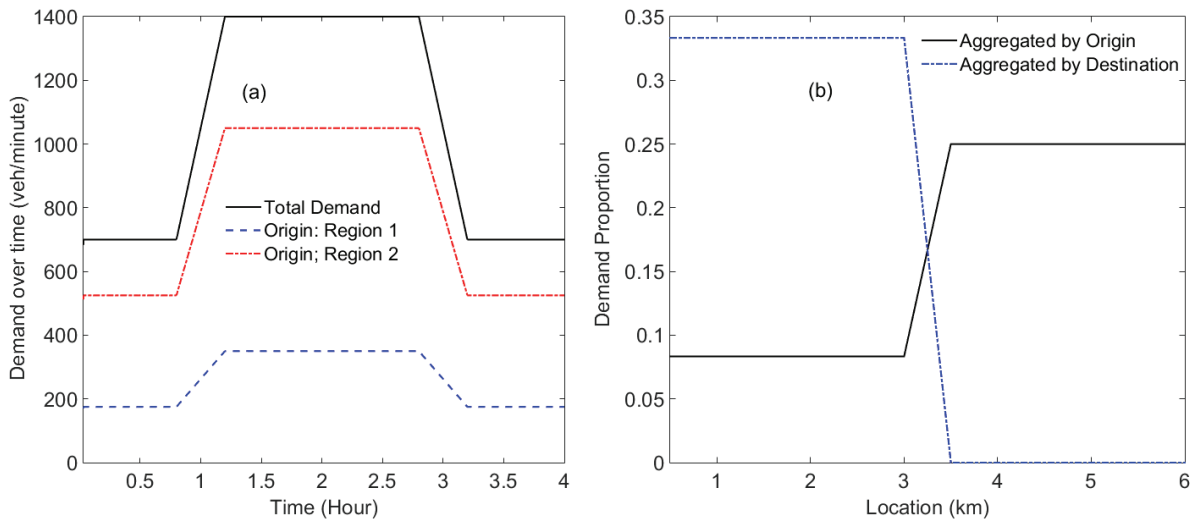


Figure 3. Demand: (a) aggregated demand over time; (b) demand distribution with respect to origins and destinations

Furthermore, trip length for a given origin-destination pair (x_o, x_d) is determined as follows:

⁹ People's learning behavior and mode choices will rely on at least their socioeconomics characteristics and psychology etc. (this might be measured or estimated by surveys), which goes beyond the focus of this paper. Later we will examine how the system dynamics can vary with the learning and information factors.

$$d(x_o, x_d) = \begin{cases} 1.5 \cdot (|x_o - x_d| + \min\{x_o, x_d\}) & x_o \leq R_1; x_d \leq R_1 \\ 1.5 \cdot (|x_o - R_1| + |R_1 - x_d| + \min\{R_1, x_d\}) & x_o > R_1; x_d \leq R_1 \end{cases}.$$

For $x_o > R_1$ and $x_d > R_1$, we have $d(x_o, x_d) = 1.5 \cdot |x_o - x_d|$, and for $x_o \leq R_1$ and $x_d > R_1$, we have $d(x_o, x_d) = 1.5 \cdot (|x_d - R_1| + |x_o - R_1| + \min\{R_1, x_o\})$. Therefore, $d(x_o, x_d) = d(x_d, x_o)$ will hold.

4.2. Day-to-day Dynamics

We now explore the day to day flow evolution of the doubly dynamical system. The parking prices are initially set to $p_1 = 6$ (EUR) and $p_2 = 2$ (EUR) respectively. Particularly, we test the day to day evolution process under different initial non-equilibrium flow solutions (by solution, we mean both the modal-split and roadway traffic pattern). Suppose the equilibrium travel cost of mode m for travelers with an origin-destination pair (x_o, x_d) and a departure time of t is

$C_m^{e,*}(x_o, x_d, t) = C_m^{p,*}(x_o, x_d, t)$. To generate a non-equilibrium solution, we let

$$C_m^p(x_o, x_d, t) = C_m^{p,*}(x_o, x_d, t) \cdot (1 + \varphi),$$

where φ is uniformly distributed on $[-0.3, 0.3]$ for the numerical analysis.

In order to verify the convergence (from different initial flow pattern solutions) to the identical equilibrium state, we examine the errors (or discrepancy) between the traffic pattern on a day and that at the equilibrium solution. In particular, the percentage errors (mean and max) are defined as follows. Suppose at the user equilibrium, the modal-split is $\delta_m^*(x_o, x_d, t)$ for all x_o, x_d and t . The ‘‘Mean’’ of percentage error is

$$e_{mean} = \frac{\int_{t_s}^{t_e} \int_0^{R_1} \int_{R_1}^R \frac{\sum_{m \in \{a, t, p\}} |\delta_m(x_o, x_d, t) - \delta_m^*(x_o, x_d, t)|}{\delta(x_o, x_d, t)} dx_o dx_d dt}{R_1 \cdot R \cdot (t_e - t_s)} + \frac{\int_{t_s}^{t_e} \int_0^{R_1} \int_0^{R_1} \frac{\sum_{m \in \{a, t\}} |\delta_m(x_o, x_d, t) - \delta_m^*(x_o, x_d, t)|}{\delta(x_o, x_d, t)} dx_o dx_d dt}{R_1 \cdot R \cdot (t_e - t_s)}, \quad (31)$$

Indeed e_{mean} is the average percentage error (regarding modal-split) over (x_o, x_d, t) , while the ‘‘Max’’ value e_{max} is the maximum percentage error if we go through all combinations of (x_o, x_d, t) . It is obvious that $e_{mean} \leq e_{max}$. As the above errors go to zero, the equilibrium modal-

split is achieved, as well as for the dynamic traffic pattern in the network. Note that while Eq.(31) is in continuous forms, it should be changed accordingly to account for the discretization of space and time in the numerical experiments.

Following the above, Figure 4(a) and Figure 4(b) display the convergence of the model to identical equilibrium state (fixed point) after day-to-day evolution under different initial solutions. Specifically, Figure 4(a) shows how individual perceived costs (solid lines) and experienced costs (dash lines) will evolve over (calendar) time under different initial state (or solution). Particularly, travelers with O-D pair (10, 2) and departure times 1.2, 2.25 and 3.5 hour respectively are taken as an example (time points of 1.2, 2.25, and 3.5 hour can be regarded as onset of congestion, middle of congested period, and offset of congestion receptively). Furthermore, Figure 4(b) shows how the discrepancy between the demand pattern on the day and the equilibrium pattern evolves over days.

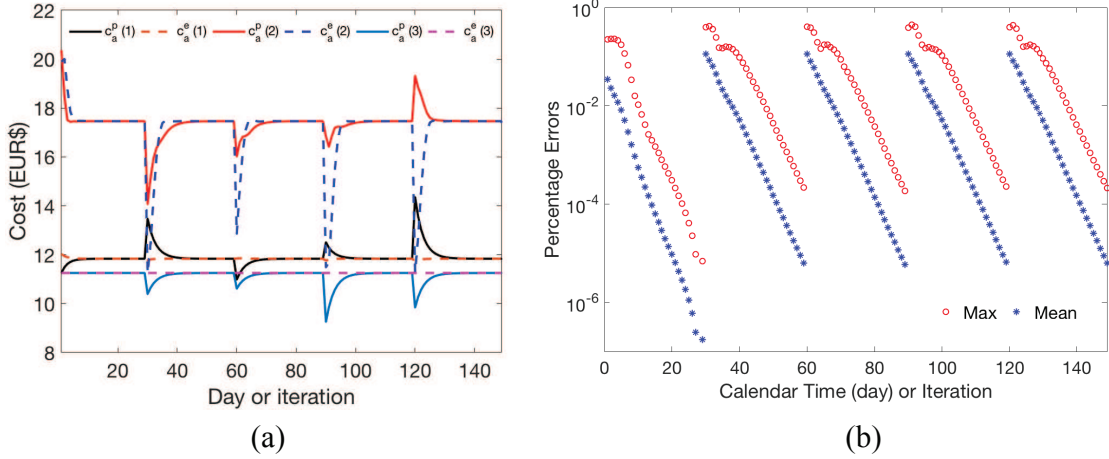


Figure 4. Day to day evolution: (a) Auto costs evolution for O-D pair (10, 2) and departure time at 1.2 hour (1), at 2.25 hour (2), and at 3.5 hour (3); (b) Errors evolution over days/iterations

We start from day zero (the x-axis is the calendar time) with a non-equilibrium initial solution (and then for every 30 days we generate a different non-equilibrium solution). As can be seen in Figure 4(a), after less than 10 days/iterations, the perceived and experienced travel costs for the same travelers evolve to the same value, and system reaches the equilibrium state. Moreover, on day/iteration 31, 61, 91, 121, different non-equilibrium initial solutions are generated to test convergence under different initial conditions. As can be seen in Figure 4(a), auto cost evolves to the identical equilibrium cost under different initial states. Note that, since we have time-varying demand within a day, travel cost at onset of congestion, at middle of congested period, and at offset of congestion are different (refer to Figure 4, those departing at the middle of congestion experience much higher travel cost).

While Figure 4(a) only shows evolutions of individual travel costs, Figure 4(b) further verifies the convergence to the identical equilibrium state by examining the errors (or discrepancy) between the traffic pattern on a day and that at the equilibrium solution. It is evident in Figure 4(b) that different non-equilibrium initial solutions will all evolve to the identical equilibrium solution (indeed we have tried many more initial solutions while we only plot those in Figure 4 for illustration).

Now we turn to investigate how the learning factor ω and information factor ρ could affect the day-to-day evolution. The learning factor should be within the range of $[0,1]$, and the information factor should be positive. Numerical tests are conducted for many combinations of (ω, ρ) , and we take seven pairs as illustrative examples, which are $(0.3, 1.0)$, $(0.5, 1.0)$, $(0.7, 1.0)$, $(0.9, 1.0)$, $(0.7, 0.15)$, $(0.7, 0.5)$, $(0.7, 1.0)$, and $(0.7, 1.5)$. Note that in practice these factors need to be estimated with data (through, e.g., maximum likelihood estimation, see, e.g., [Xiao and Lo, 2016](#)).

Figures 5(a), 5(b), 5(c) and 5(d) display how individual auto costs (perceived cost and experienced cost) evolve over days under different learning factors (but with identical information factor of 1.0). Figures 5(c), 5(e), 5(f), and 5(g) display how individual auto costs evolve over days under different information factors (but with identical learning factor of 0.7). Figure 5(h) further displays how the errors (mean values) defined before evolve over days (or iterations) for different combinations of (ω, ρ) . Note that we take travelers with O-D pair $(10, 2)$ and departure time at $t = 3.0$ hours as illustrative examples.

It is evident in Figure 5 that, given the same information factor of 1.0, as the learning factor increases from 0.3 to 0.9 (less and less weight has been put on previous single day's experience), the fluctuation on cost decreases. This is because, a larger learning factor indicates that travelers rely on single day's experience less, and rely on perception (from long term experience) more. However, a larger learning factor does not mean a faster convergence, i.e., a too small learning factor (0.3) leads to frequent fluctuation, and a too large learning factor (0.9) leads to ineffective or conservative updating of perceived cost. This is also consistent with the errors evolution in Figure 5(h) where the cases under learning factors of 0.5 and 0.7 have faster convergence than those under 0.3 or 0.9 (we only display the average percentage error here).

A large learning factor is likely to lead to convergence, because travelers are insensitive to a single day's experience. However, if we have a very small learning factor, e.g., 0.1, which means that travelers are very sensitive to single day's experience, the fluctuation in cost (as well as

modal-split) can be significant, and system never converges to an equilibrium state, but oscillates from day to day (we have tested this but omit detailed discussions).

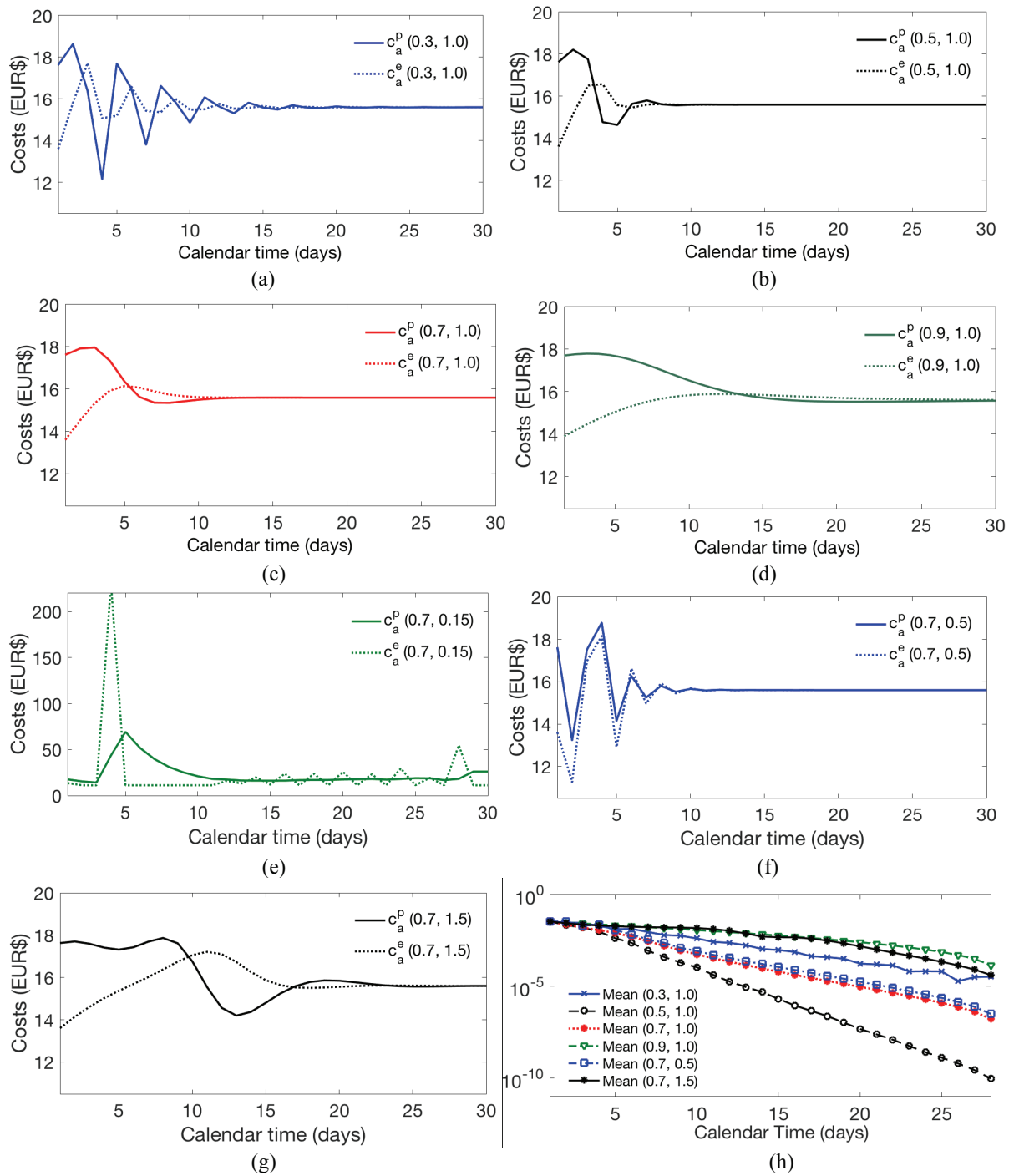


Figure 5. Evolution under different pairs of (ω, ρ) : (a)-(g) Auto cost (O-D pair (10, 2) and departure time at 3 hour); (h) Errors in modal-split

Now we further compare Figures 5(c), 5(e), 5(f), and 5(g), where we fix the learning factor at 0.7, and change the information parameter. Note that $\rho = 1$ means that the exact cost difference (between cost predictions of the current day and the previous day) based on “current condition” is taken into account.

As can be seen, a smaller information factor leads to a larger “frequency” in fluctuation (i.e., more frequent shift between crest and trough). Note that a large factor (1.5) and a small factor (0.5) can lead to large variations. This is also consistent with Figure 6(h) where cases with information factor 1.0 has faster convergence than those for 0.5 and 1.5 (learning factor is fixed at 0.7).

Figure 5(e) shows the case with an information factor of 0.15, which leads to frequent fluctuation and non-convergence. This means that, when travelers have less information or are insensitive to real-time traffic information, we might expect more variations. This highlights the importance of providing information to travelers, not only to help reduce cost by selecting the best mode and route, but also to stabilize the system (please also refer to the discussion of learning model in Eq.(10)). Furthermore, Figure 5(e) indicates that most existing day-to-day models in the literature with static traffic model for single day (corresponds to $\rho = 0$) is unlikely to have convergence if we consider dynamic traffic in a day. With the current day-to-day learning model as a starting point, future study will try to look for more analytical tractable models to examine the “dynamics of dynamics”.

4.3. Period-to-period Adaptive Pricing

Now we show the performance of the period-to-period adaptive parking pricing strategy under the demand given in Figure 3(a). The price adjustment factors are $p_{1,0} = 4 \times 10^{-4}$ and $p_{2,0} = 2 \times 10^{-4}$. Note that each period is 30 days. For comparison purpose, we choose three initial price solutions for (p_1, p_2) , i.e., (4,1); (6,2); (10,5) (unit is EUR\$). And in Figure 7, the three different initial prices are referred as (1), (2) and (3).

Figure 6(b) shows how parking pricing evolves over periods, and Figure 6(a) shows how the total costs (both user cost and social cost) evolve over days. As can be seen, while the initial prices are different, they all converge to similar values (i.e., 8.5 for p_1 and 2.0 for p_2). We also notice that, in the first three or four periods, the price adjustments are relatively large. After that the prices already become quite close to the final values. It means that this framework can achieve good performance in a relatively short time. Indeed, the social cost reduction and oscillation both

decrease with periods, and approach zero in the end. The total social cost reduction, as can be seen in Figure 6(a), i.e., the solid lines, depends on the initial system state. Unsurprisingly, lower initial prices indicate more congested system thus larger social cost reduction in the end. However, the total user cost (dash-dot lines in Figure 6(a)) increases in case (1) and case (2).¹⁰

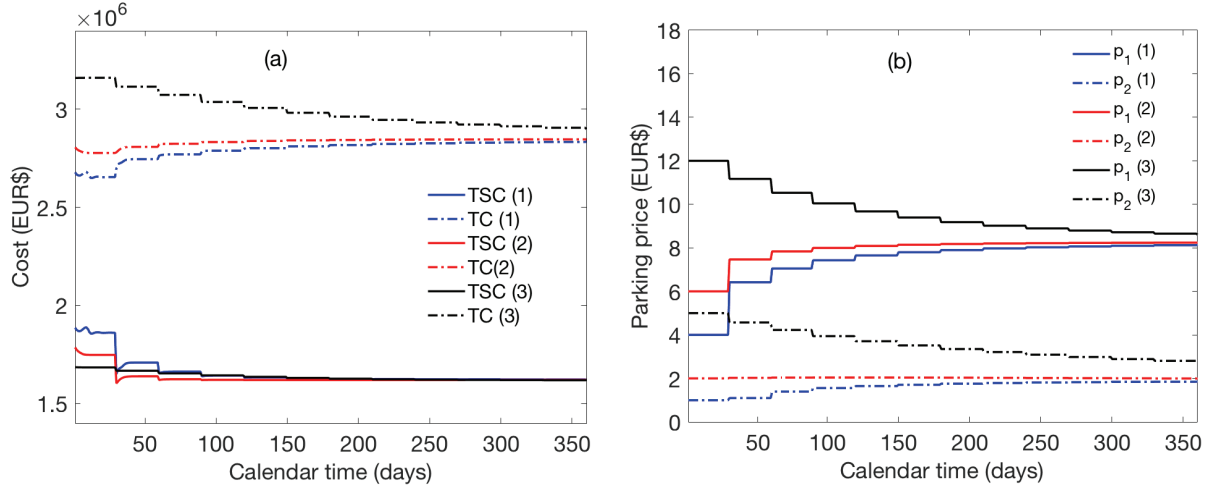


Figure 6. Adaptive pricing and costs evolution under three different initial prices

Figure 7 further shows how the individual travel cost (auto mode as an example) and modal-split evolve over periods. Note that there are larger cost fluctuations during the first period (see Figure 7(a)). This is because, the initial solution is a bit further away from the equilibrium state, while for the later periods, the initial state (at the beginning of each period) is an equilibrium solution from last period. As the prices do not change too sharply, such a solution will not be far from the equilibrium solution for the new prices. Due to this reason, we also see decreasing fluctuations and increasing convergence speed for later periods since the price adjustments become smaller and smaller. In Figure 7(a), we also see that after 6 periods (180 days), perceived cost, experienced costs and predicted cost based on “current condition” all approach the same value. This is because as congestion diminishes, speed becomes constant over time, thus cost estimate/prediction based on “current condition” becomes very accurate.

¹⁰ Given the same numerical setting, the minimum social cost (cost currency: EUR) of 1.56×10^6 is indeed achieved at price pair (10.4, 5.0), and the corresponding total user cost is 3.08×10^6 . As can be observed the Figure 6(a), our adaptive pricing reach a minimum social cost of 1.61×10^6 at price pair (8.4, 2.0), and the corresponding total user cost is 2.84×10^6 . We would like to highlight that the adaptive pricing can achieve similar efficiency as the possible minimum (loses 3%), but lead to a much lower total user cost, which is around 15% of the minimum social cost. This is because that the travelers pay much less, i.e., (8.4, 2.0) vs. (10.4, 5.0). Besides, it is worth mentioning that the 3% gain from larger prices is due to that park-and-ride mode becomes an inefficient mode (with additional transfer cost) when there is very light congestion in the city center.

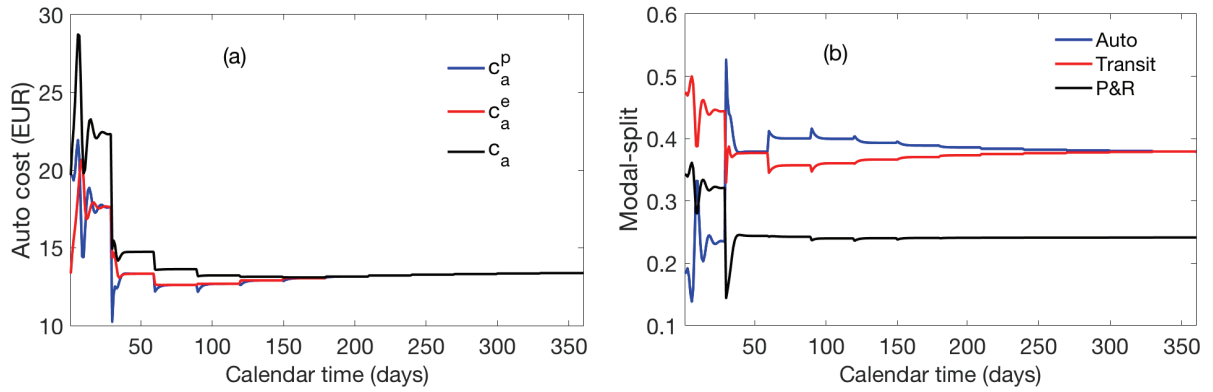


Figure 7. Individual cost and modal-split evolutions over period: initial prices (4, 1); O-D pair (10, 2) and departure time at 2.25 hour

We further visualize diminishing congestion in Figure 8(a), where the Region 1 (city center) speed over (clock) time is displayed against the days (thus we present both day-to-day and within-day dynamics). The figure presents contour plots of speed and accumulation for both within-day and day-to-day evolution. As can be seen, the system is quite congested in the beginning (period 1: day 1 to day 30, please refer to the blue bands in the speed figure, which means that speed is within the range of [5, 10]). Over days, as we adjust the pricing, congested duration becomes shorter and congestion becomes less severe. This speed evolution corresponds to the regional accumulation evolution displayed in Figure 8(b).

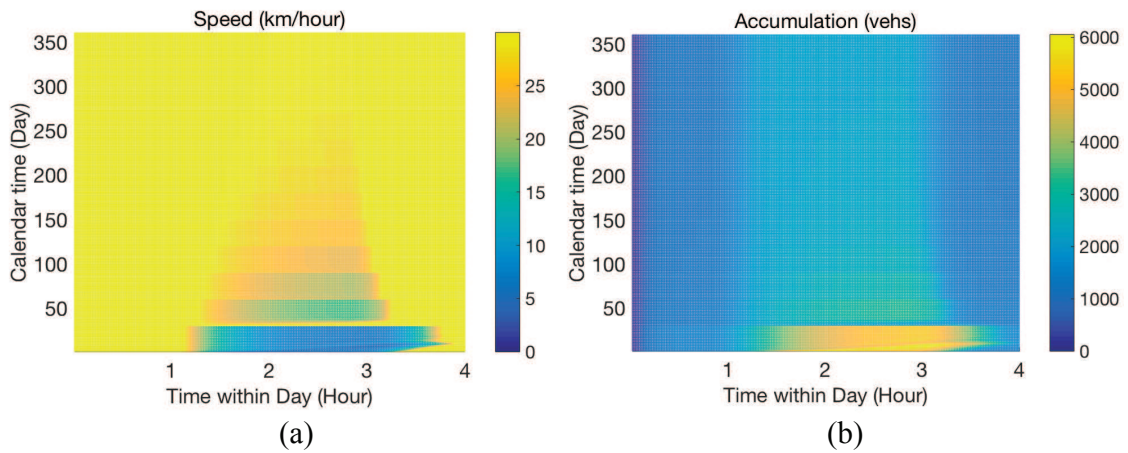


Figure 8. Speeds and accumulations evolutions over days: initial prices (4, 1)

To this point, we assume that demand is deterministic, under which equilibrium state can exist. However, in reality travel demand fluctuates from day to day, even it follows a recurrent trend. In this section, we consider that the total demand profile in Figure 3 is the average value. Every day for a time step (within-day), the demand profile in Figure 3 is subject to a uniformly variation within the range of [-10%, 10%]. Figure 9(a) is the realized demand in one single day.

In this case, there will be no such equilibrium as described in Section 3 since the demand realization on each day is random and different. However, as the demand still follows the similar pattern from day to day, we expect that the adaptive pricing can still guide the system into an efficient state. This is because, although there is not an equilibrium anymore, the dynamic traffic pattern in the end of a period will be close to the equilibrium state. We start from the parking price pair (4, 1), and adopt the similar strategy as before. However, now the price adjustments will not be based on conditions at an equilibrium state, but with certain levels of variation. Since at the end of a period, the system state is close to equilibrium state, parking price adjustments are very close to that with deterministic demand (we omit the details as it is very similar to that in Figure 6(b)). Moreover, the total social cost and total user cost follow similar trend with those under deterministic demand case, but with small variations, which are shown in Figure 9(b).

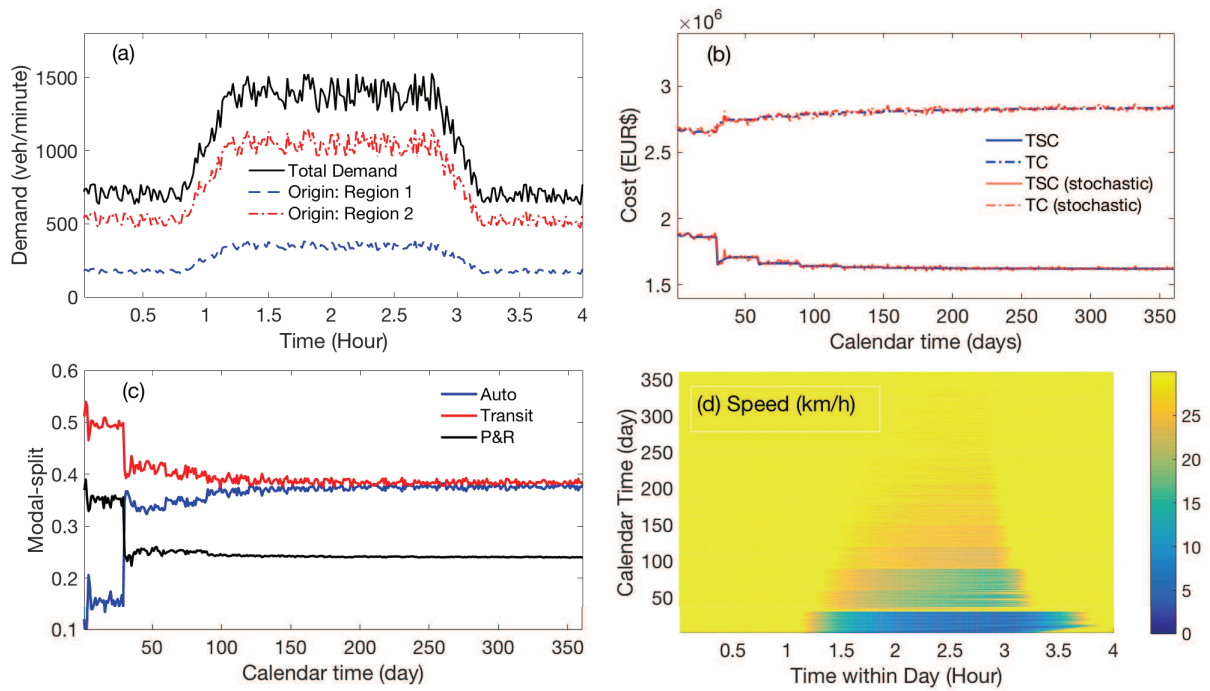


Figure 9. Stochastic demand case: (a) realized demand for one day; (b) costs evolution: deterministic vs. stochastic; (c) modal-split (O-D: (10, 2) & departure time: 2.25 hours); (d) speed (Region 1) evolution over time

We also show the evolution of modal-split (for O-D pair (10, 2) and departure time at 2.25 hours) in Figure 9(c), and the speed (for Region 1) evolution over time in Figure 9(d), given the stochastic demand. Not surprisingly, they also follow similar trends with those under deterministic demand. Note that, we do not show the individual travel cost evolution and the accumulation evolution as they are also quite similar to those under deterministic demand case.

The above results indicate that the adaptive pricing framework is promising for practice as it can still effectively guide the system to uncongested state under demand uncertainty. Its performance is robust to certain levels of demand variations. Moreover, if the roadway network is already very congested under deterministic demand, allowing very large variations of demand (e.g., 30% rather than 10%) may lead to network gridlock situations for some durations. However, the adaptive pricing strategy (through increasing pricing when facing gridlock) indeed can eliminate gridlock and guide the system to uncongested state.

5. Conclusion

This study proposes a model for multi-region and multi-modal transportation systems, given that the travelers can adapt their mode choices from day to day, and the network traffic dynamics in a day evolve over (calendar) time. Firstly, this paper contributes to the literature by incorporating realistic within-day network traffic dynamics into a day-to-day modeling framework. Particularly, we incorporate real-time information's impacts on people's choices and on the evolution of traffic over days. Secondly, the aggregated traffic modeling approach in the paper provides flexibility and capability for modeling integrated large-scale city networks, where both multi-modality and inter-modality exist. Thirdly, we propose an adaptive pricing strategy to guide the system to a more efficient state, which is practical and suitable for implementation in large-scale networks. Particularly important is that the adaptive strategy mainly relies on network traffic variables observable in practice. Fourthly, extensive numerical experiments have been conducted to show convergence of the day to day evolution model and its sensitivity to the learning factor and the information factor. Also, efficiency of the proposed adaptive pricing is examined for both deterministic and stochastic demand cases with numerical experiments.

Future study will take into account route choice and/or departure time choice into the model besides mode choices. Firstly, when travelers can also adapt their route choices from day to day, the trip length for given origin-destination can vary over days (unlike the constant trip length in this study). This problem requires one more level of formulation regarding route choices (for MFD-based model with route choices, one may refer to, e.g., [Yildirimoglu et al., 2015](#)). Secondly, this study assumes that the demand over time is given (but is time-varying), i.e., departure time choices are not considered. We may incorporate activity start time for travelers, as well as schedule penalties for unpunctuality in the travel cost formulation (similar to, e.g., [Vickrey, 1969](#); [Xiao and Lo, 2016](#)), thus can model day-to-day departure time choices evolution. While these directions might further complexify the dynamics of the problem, they can still provide a more elegant environment compared to very detailed simulations, and conclusions with physical

interpretations can be made. Last but not the least, a behavioral analysis to calibrate some of the parameters presented in the model could also be of some scientific interests, especially for researchers in this area.

Acknowledgement. This research was supported by ERC Starting Grant “META FERW: Modeling and controlling traffic congestion and propagation in large-scale urban multimodal networks”. The authors thank the three anonymous reviewers for their constructive comments.

Reference

- Arnott, R., 2013. A bathtub model of downtown traffic congestion. *Journal of Urban Economics*, 76, pp.110-121.
- Ben-Akiva, M., De Palma, A. and Kanaroglou, P., 1986. Dynamic model of peak period traffic congestion with elastic arrival rates. *Transportation Science*, 20(3), pp.164-181.
- Bie, J. and Lo, H.K., 2010. Stability and attraction domains of traffic equilibria in a day-to-day dynamical system formulation. *Transportation Research Part B: Methodological*, 44(1), pp.90-107.
- Cantarella, G.E. and Cascetta, E., 1995. Dynamic processes and equilibrium in transportation networks: towards a unifying theory. *Transportation Science*, 29(4), pp.305-329.
- Cantarella, G.E., Velonà, P. and Watling, D.P., 2015. Day-to-day dynamics & equilibrium stability in a two-mode transport system with responsive bus operator strategies. *Networks and Spatial Economics*, 15(3), pp.485-506.
- Cascetta, E., Nuzzolo, A., Russo, F. and Vitetta, A., 1996. A modified logit route choice model overcoming path overlapping problems: specification and some calibration results for interurban networks. In *Proceedings of the 13th International Symposium on Transportation and Traffic Theory* (pp. 697-711). Oxford, NY, USA: Pergamon.
- Chiabaut, N., 2015. Evaluation of a multimodal urban arterial: The passenger macroscopic fundamental diagram. *Transportation Research Part B: Methodological*, 81, pp.410-420.
- Chiabaut, N., Xie, X. and Leclercq, L., 2014. Performance analysis for different designs of a multimodal urban arterial. *Transportmetrica B: Transport Dynamics*, 2(3), pp.229-245.
- Daganzo, C.F. and Sheffi, Y., 1977. On stochastic models of traffic assignment. *Transportation Science*, 11(3), pp.253-274.
- Friesz, T.L., Bernstein, D., Mehta, N.J., Tobin, R.L. and Ganjalizadeh, S., 1994. Day-to-day dynamic network disequilibria and idealized traveler information systems. *Operations Research*, 42(6), pp.1120-1136.

- Geroliminis, N. and Daganzo, C.F., 2008. Existence of urban-scale macroscopic fundamental diagrams: Some experimental findings. *Transportation Research Part B: Methodological*, 42(9), pp.759-770.
- Geroliminis, N., Zheng, N. and Ampountolas, K., 2014. A three-dimensional macroscopic fundamental diagram for mixed bi-modal urban networks. *Transportation Research Part C: Emerging Technologies*, 42, pp.168-181.
- Gonzales, E.J. and Daganzo, C.F., 2012. Morning commute with competing modes and distributed demand: user equilibrium, system optimum, and pricing. *Transportation Research Part B: Methodological*, 46(10), pp.1519-1534.
- Guo, R.Y., Yang, H., and Huang, H.J., 2017. Are we really solving the dynamic traffic equilibrium problem with a departure time choice? *Transportation Science*, accepted.
- Guo, R.Y., Yang, H., Huang, H.J. and Tan, Z., 2015. Day-to-day flow dynamics and congestion control. *Transportation Science*, 50(3), pp.982-997.
- Guo, X. and Liu, H.X., 2011. Bounded rationality and irreversible network change. *Transportation Research Part B: Methodological*, 45(10), pp.1606-1618.
- He, X. and Liu, H.X., 2012. Modeling the day-to-day traffic evolution process after an unexpected network disruption. *Transportation Research Part B: Methodological*, 46(1), pp.50-71.
- Horowitz, J.L., 1984. The stability of stochastic equilibrium in a two-link transportation network. *Transportation Research Part B: Methodological*, 18(1), pp.13-28.
- Lamotte, R. and Geroliminis, N., 2016. The Morning Commute in Urban Areas: Insights from Theory and Simulation. In *Transportation Research Board 95th Annual Meeting (No. 16-2003)*.
- Li, X. and Yang, H., 2016. Dynamics of modal choice of heterogeneous travelers with responsive transit services. *Transportation Research Part C: Emerging Technologies*, 68, pp.333-349.
- Liu, T.L., Huang, H.J., Yang, H. and Zhang, X., 2009. Continuum modeling of park-and-ride services in a linear monocentric city with deterministic mode choice. *Transportation Research Part B: Methodological*, 43(6), pp.692-707.
- Liu, W. and Geroliminis, N., 2016. Modeling the morning commute for urban networks with cruising-for-parking: an MFD Approach. *Transportation Research Part B: Methodological*, 93, pp.470-494.
- Liu, W., Yang, H. and Yin, Y., 2014. Traffic rationing and pricing in a linear monocentric city. *Journal of Advanced Transportation*, 48(6), pp.655-672.
- Mahmassani, H.S. and Chang, G.L., 1987. On boundedly rational user equilibrium in transportation systems. *Transportation Science*, 21(2), pp.89-99.

- Mariotte, G., Leclercq, L. and Laval, J.A., 2017. Dual expression of macroscopic urban models: Analytical and numerical investigations with piecewise linear functions. In Transportation Research Board 96th Annual Meeting (No. 17-04928).
- Nagurney, A., 1993. Network economics: A variational inequality approach. Springer Science & Business Media.
- Nagurney, A. and Zhang, D., 1997. Projected dynamical systems in the formulation, stability analysis, and computation of fixed-demand traffic network equilibria. *Transportation Science*, 31(2), pp.147-158.
- Pineda, C., Cortés, C.E., Jara-Moroni, P. and Moreno, E., 2016. Integrated traffic-transit stochastic equilibrium model with park-and-ride facilities. *Transportation Research Part C: Emerging Technologies*, 71, pp.86-107.
- Ramezani, M., Haddad, J. and Geroliminis, N., 2015. Dynamics of heterogeneity in urban networks: aggregated traffic modeling and hierarchical control. *Transportation Research Part B: Methodological*, 74, pp.1-19.
- Saeedmanesh, M. and Geroliminis, N., 2016. Clustering of heterogeneous networks with directional flows based on “Snake” similarities. *Transportation Research Part B: Methodological*, 91, pp.250-269.
- Sandholm, W.H., 2002. Evolutionary implementation and congestion pricing. *The Review of Economic Studies*, 69(3), pp.667-689.
- Smith, M.J., 1984. The stability of a dynamic model of traffic assignment-an application of a method of Lyapunov. *Transportation Science*, 18(3), pp.245-252.
- Smith, M.J. and Mounce, R., 2011. A splitting rate model of traffic re-routing and traffic control. *Transportation Research Part B: Methodological*, 45(9), pp.1389-1409.
- Smith, M.J. and Watling, D.P., 2016. A route-swapping dynamical system and Lyapunov function for stochastic user equilibrium. *Transportation Research Part B: Methodological*, 85, pp.132-141.
- Smith, M.J. and Wisten, M.B., 1995. A continuous day-to-day traffic assignment model and the existence of a continuous dynamic user equilibrium. *Annals of Operations Research*, 60(1), pp.59-79.
- Tan, Z., Yang, H. and Guo, R.Y., 2015. Dynamic congestion pricing with day-to-day flow evolution and user heterogeneity. *Transportation Research Part C: Emerging Technologies*, 61, pp.87-105.
- Tsekeris, T. and Geroliminis, N., 2013. City size, network structure and traffic congestion. *Journal of Urban Economics*, 76, pp.1-14.
- Verhoef, E.T., 2005. Second-best congestion pricing schemes in the monocentric city. *Journal of Urban Economics*, 58(3), pp.367-388.

- Vickrey, W.S., 1969. Congestion theory and transport investment. *American Economic Review*, 59(2), pp.251-260.
- Wang, J.Y., Yang, H. and Lindsey, R., 2004. Locating and pricing park-and-ride facilities in a linear monocentric city with deterministic mode choice. *Transportation Research Part B: Methodological*, 38(8), pp.709-731.
- Wardrop, J.G., 1952. Some theoretical aspects of road traffic research. *Proceedings of the Institution of Civil Engineers*, pp.325-362.
- Watling, D., 1999. Stability of the stochastic equilibrium assignment problem: a dynamical systems approach. *Transportation Research Part B: Methodological*, 33(4), pp.281-312.
- Watling, D. and Hazelton, M.L., 2003. The dynamics and equilibria of day-to-day assignment models. *Networks and Spatial Economics*, 3(3), pp.349-370.
- Xiao, F., Yang, H. and Ye, H., 2016. Physics of day-to-day network flow dynamics. *Transportation Research Part B: Methodological*, 86, pp.86-103.
- Xiao, L. and Lo, H.K., 2015. Combined route choice and adaptive traffic control in a day-to-day dynamical system. *Networks and Spatial Economics*, 15(3), pp.697-717.
- Xiao, Y. and Lo, H.K., 2016. Day-to-day departure time modeling under social network influence. *Transportation Research Part B: Methodological*, 92, pp.54-72.
- Yang, F., Yin, Y. and Lu, J., 2007. Steepest descent day-to-day dynamic toll. *Transportation Research Record: Journal of the Transportation Research Board*, (2039), pp.83-90.
- Ye, H. and Yang, H., 2013. Continuous price and flow dynamics of tradable mobility credits. *Transportation Research Part B: Methodological*, 57, pp.436-450.
- Ye, H., Yang, H. and Tan, Z., 2015. Learning marginal-cost pricing via a trial-and-error procedure with day-to-day flow dynamics. *Transportation Research Part B: Methodological*, 81, pp.794-807.
- Yildirimoglu, M. and Geroliminis, N., 2013. Experienced travel time prediction for congested freeways. *Transportation Research Part B: Methodological*, 53, pp.45-63.
- Yildirimoglu, M., Ramezani, M. and Geroliminis, N., 2015. Equilibrium analysis and route guidance in large-scale networks with MFD dynamics. *Transportation Research Part C: Emerging Technologies*, 59, pp.404-420.
- Zhang, F., Lindsey, R. and Yang, H., 2016. The Downs-Thomson paradox with imperfect mode substitutes and alternative transit administration regimes. *Transportation Research Part B: Methodological*, 86, pp.104-127.
- Zhang, F., Yang, H. and Liu, W., 2014. The Downs-Thomson Paradox with responsive transit service. *Transportation Research Part A: Policy and Practice*, 70, pp.244-263.
- Zheng, N. and Geroliminis, N., 2013. On the distribution of urban road space for multimodal congested networks. *Transportation Research Part B: Methodological*, 57, pp.326-341.

- Zheng, N. and Geroliminis, N., 2016. Modeling and optimization of multimodal urban networks with limited parking and dynamic pricing. *Transportation Research Part B: Methodological*, 83, pp.36-58.
- Zhou, Z., Chen, A. and Bekhor, S., 2012. C-logit stochastic user equilibrium model: formulations and solution algorithm. *Transportmetrica*, 8(1), pp.17-41.